Journal of Physics: Conference Series **501** (2014) 012023 doi:10.1088/1742-6596/501/1/012023

Characterization of a mini-channel heat exchanger for a heat pump system

A Arteconi[1,3], G Giuliani[2], M Tartuferi[2] and F Polonara[2]
[1]Università degli Studi eCampus, via Isimbardi 10, Novedrate (CO), 22060, Italy
[2]Università Politecnica delle Marche, Dipartimento di Ingegneria Industriale e Scienze Matematiche, via Brecce Bianche 1, Ancona, 60131, Italy

E-mail: a.arteconi@univpm.it

Abstract. In this paper a mini-channel aluminum heat exchanger used in a reversible heat pump is presented. Mini-channel finned heat exchangers are getting more and more interest for refrigeration systems, especially when compactness and low refrigerant charge are desired. Purpose of this paper was to characterize the mini-channel heat exchanger used as evaporator in terms of heat transfer performance and to study the refrigerant distribution in the manifold. The heat exchanger characterization was performed experimentally by means of a test rig built up for this purpose. It is composed of an air-to-air heat pump, air channels for the external and internal air circulation arranged in a closed loop, measurement sensors and an acquisition system. The overall heat transfer capacity was assessed. Moreover, in order to characterize the flow field of the refrigerant in the manifold of the heat exchanger, a numerical investigation of the fluid flow by means of CFD was performed. It was meant to evaluate the goodness of the present design and to identify possible solutions for the future improvement of the manifold design.

1. Introduction

Mini-channel finned heat exchangers are getting more and more interest for refrigeration systems, especially when compactness and low refrigerant charge are desired [1]. Several studies investigated performance and operative characteristics of such systems. Many authors presented heat transfer and pressure drops correlations [2 - 7]. In particular maldistribution of the refrigerant is a challenge in this type of heat exchangers, especially for evaporators where the entering fluid is usually in two-phase condition. The design of the distribution manifold plays an important role in how the gas and liquid phases distribute, together with pressure drops in the manifold and air distribution on the external side [8]. Among the main findings in the literature, Kulkarni et al. [9] found that mass flow maldistribution cannot be controlled through changing either the port/header diameter or the refrigerant state, but it can only be controlled by minimizing pressure gradients along header. Regarding the inlet configuration, Kim et al. [10] stated that the best gas distribution is obtained for normal inlet configuration, followed by vertical and parallel inlet configuration, and the effect of mass flow or quality on gas distribution is not significant. Moreover the protrusion of multiports into the header makes incoming liquid bypass the frontal channels yielding better flow distribution [11]. Qi et al. [12] studied the effect of fin shape, revealing that the louver fin which is flat at fin top is more suitable for mini-channel evaporator than corrugated louver fin in reduction of air side pressure drop and, for the

[3] To whom any correspondence should be addressed.

same purpose, a simpler refrigerant side flow path arrangement is preferable. However the main effect on heat exchange is due to the refrigerant maldistribution more than air maldistribution (30% performance reduction against 9% respectively) [13], even if both aspects have to be taken into account. Different approaches were used in the abovementioned works, based on experimental tests and/or numerical simulations, among them Selleri et al. [14] developed a multi-objective optimization to find the best design configuration for a mini-channel heat exchanger.

Purpose of this paper was to characterize the mini-channel heat exchanger used as evaporator in terms of heat transfer performance and to study the refrigerant distribution in the manifold. The heat exchanger characterization was performed experimentally by means of a test rig built up for this purpose. Moreover, in order to characterize the flow field of the refrigerant in the manifold of the heat exchanger, a numerical investigation of the fluid flow by means of CFD was performed. It was meant to evaluate the goodness of the present design with the main objective of identifying useful aspects for the future improvement of the manifold design.

2. Experimental investigation

The heat exchanger characterization was performed experimentally by means of a test rig built up for this purpose. It is composed of an air-to-air heat pump, air channels for the external and internal air circulation arranged in a closed loop, measurement sensors and an acquisition system. In the following sections a detailed description of the test rig and of the obtained results is provided.

2.1. The test rig set up

The test rig is composed of an-to-air reversible heat pump, using R410A as refrigerant fluid, with air channels for the external and internal air circulation arranged in a closed loop. In figure 1 a schematic (a) and a 3D layout (b) of the test rig are shown. The channels are made of expanded polyurethane covered with aluminum sheets, that provides thermal insulation and avoids air leakages. The air is blown inside the channels by means of fans. The fan on the indoor side is provided with an inverter, thus it is possible to vary the air flow rate for the experimental tests purposes. The aim of the closed air channel circuits is to simulate the indoor and outdoor environment. Each channel collects the air at the outlet of the heat pump and, depending on the considered side (outdoor or indoor) and operative mode (heating or cooling), heats or cools it up to the necessary inlet conditions and then sends it back into the heat pump. In this way it is possible to test the system at different outdoor and indoor conditions. The air heating inside the channels is made by means of a 12kW electric resistance, while the air cooling by means of a water cooling circuit. Both the systems are regulated with a PID controller that keeps the air input temperature at the desired set-point values by varying the power in the former and the water flow rate in the latter system.

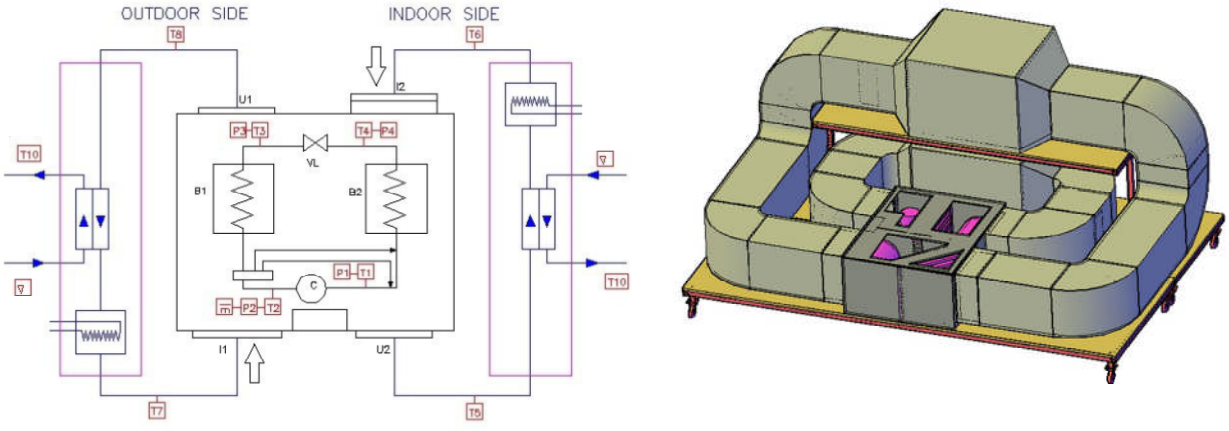

(a) (b)

Figure 1. A schematic (a) and a 3D layout (b) of the test rig.

The mini-channel heat exchanger is set inside the heat pump at the indoor side, working as evaporator or condenser on the basis of the operative mode. The test rig is equipped with different sensors (see figure 1a) in order to collect all the information about the working parameters and to assess the performance of the analyzed heat exchanger: pressure transducers on the heat pump refrigerant circuit, copper-constantan T thermocouples on the air, refrigerant and water circuits and flow meters for the refrigerant (Coriolis flow meter) and the cooling water circuits (turbine flow meter). In table 1 the sensors accuracy is reported. The data acquisition system is used to record the measurements and evaluate and control the experimental system.

Table 1. Sensors accuracy

Sensor	Accuracy
Thermocouples	± 0.5°C
Pressure transducers	1%
Turbine flow meter	1%
Coriolis flow meter	0.75%

2.2. The mini-channel heat exchanger

The heat exchanger is composed of 60 multiport extruded aluminum tubes (420 mm in height, 25 mm in width and 2 mm in thickness). Each tube consists of 15 rectangular shaped mini-channel (hydraulic diameter of a channel: 1.346 mm). Between two tubes there are corrugated fins with a pace of 1.4 mm and a thickness of 0.1 mm. The frontal area, perpendicular to the air flow, is 0.256 m^2, while the total external exchange area is 8.612 m^2 and the internal exchange area is 2.069 m^2. The heat exchanger has only one passage and at the extreme sides there are two cylindrical manifolds (diameter 33 mm) where the tubes are inserted and brazed. The heat exchanger is vertically mounted and the manifolds are horizontally placed, because for evaporator usage this configuration is preferred to facilitate the air-side condensate drainage [8]. The bottom manifold has 7 equally distributed inlets, while the top manifold has 2 outlets. The higher number of inlets is requested for a better distribution of the two phase refrigerant entering the heat exchanger working as evaporator. In figure 2 a schematic of the heat exchanger and a detail of an inlet nozzle of the bottom manifold are represented. In figure 3 a picture of the heat exchanger installed in the test rig is provided.

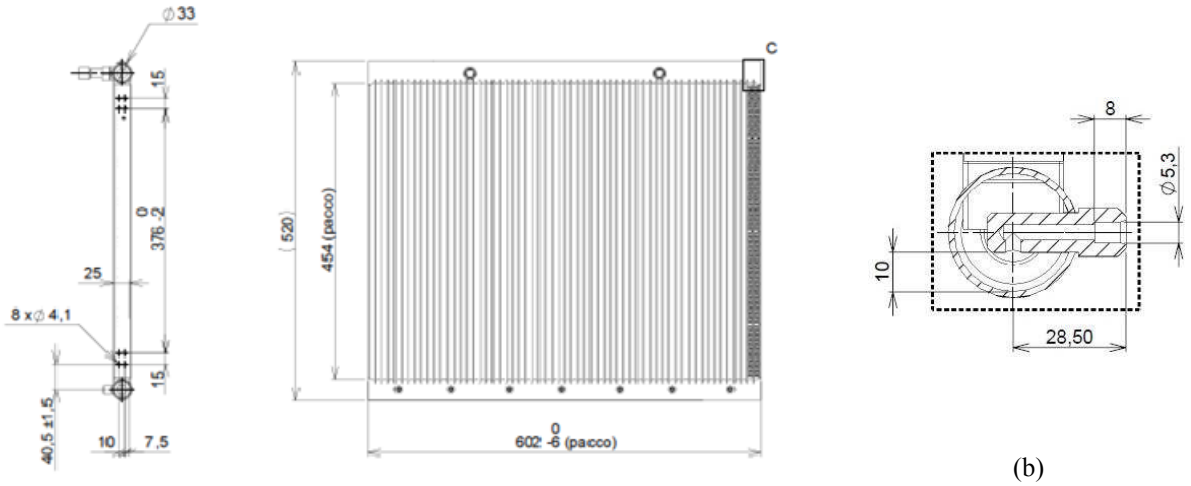

(a) (b)

Figure 2. A schematic of the mini-channel heat exchanger (a) and a detail of the inlet nozzle (b).

Figure 3. A picture of the mini-channel heat exchanger.

2.3. The experimental results

The experimental tests were aimed at characterizing the mini-channel heat exchanger into the heat pump system. The purpose was to draw curves that plot the exchanged heating rate with varying the external conditions (inlet air temperature and inlet refrigerant temperature). In this paper only the results from cooling operative mode are reported, when the mini-channel heat exchanger, set on the indoor side, plays as evaporator, that is also its most critical role.

The heat pump is an air-to-air reversible heat pump using R410A as refrigerant. In figure 4 it is possible to see the schematic of the system with the position of the installed sensors and the thermodynamic cycle on the Ph diagram. The compressor is an hermetic scroll compressor and an inverter was used during the tests to vary its speed and thus the refrigerant flow rate. The condenser is a shell and tube finned heat exchanger and a thermostatic expansion valve is employed to keep the superheating after the evaporator at the desired value (point 2 on the Ph diagram in figure 4; a further superheating up to point A is due to the four way valve before the compressor inlet).

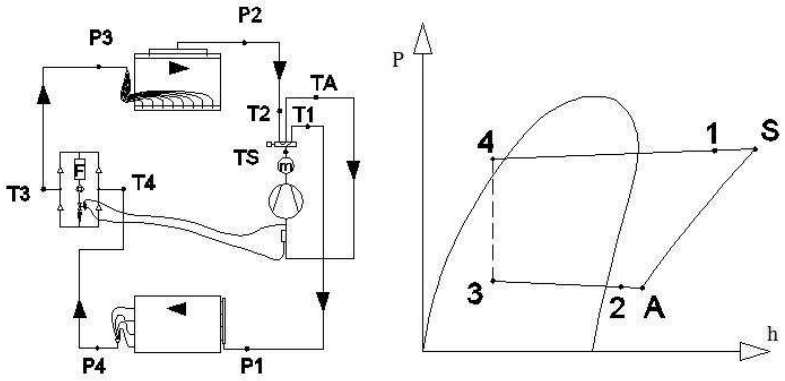

Figure 4. Heat pump schematic (a) and representation of the thermo-dynamic cycle on the Ph diagram for the cooling mode.

During the tests the superheating was kept constant to the value of 7.7°C as well as the air flow rate at the indoor side (2100 m^3/h at inverter frequency 25Hz), while the air inlet temperature at the indoor side was varied between 21°C to 27°C. Recording the refrigerant flow rate ($\dot{m}_{ref}$) and temperatures (T) and pressures (p), it was possible to calculate the heating rate exchanged in the evaporator ($\dot{P}_{ev}$) as function of the enthalpy difference (values taken from REFPROP 9.0 database [15]):

$$\dot{P}_{ev} = \dot{m}_{ref} \cdot (h_{ref,out} - h_{ref,in}) \quad (1)$$

In Table 2 some of the recorded measures are reported. Considering the sensors accuracy (Table 1) and the uncertainty of the equation of state for the refrigerant used in REFPROP [16], a relative error of 1.2% for $\dot{P}_{ev}$ was estimated using the law of error propagation.

Table 2. Experimental measurements

Test ID	T_{ev} °C	p_{ev} bar	$\dot{m}_{ref}$ kg/h	superheating °C	$\dot{w}_{air}$ m3/h	$T_{air,in}$ °C	$T_{air,out}$ °C
1	5.2	9.4	169.5	7.7	2131.5	20.9	10.6
2	9.5	10.7	154.9	7.8	2131.2	23.8	13.9
3	13.6	12.1	146.4	7.8	2148.9	27.1	17.5
4	7.5	10.1	173.2	7.6	2031.2	24.0	12.9
5	7.6	10.1	173.0	7.8	2024.6	23.9	13.0
6	3.5	8.9	180.5	7.8	1981.8	21.1	9.6
7	12.8	11.8	159.7	7.7	2191.0	26.9	17.2
8	7.1	10.0	153.2	7.9	2075.0	22.1	12.0
9	7.3	10.0	164.5	7.6	2360.0	22.0	12.9
10	11.3	11.3	149.1	7.4	2390.4	24.0	15.7

Plotting the heating rate exchanged in the evaporator versus the air inlet temperature and the difference between the air inlet temperature and the refrigerant evaporating temperature, it was assessed an equation for the interpolating surface:

$$\dot{P}_{ev} = a + b \cdot T_{in} + c \cdot \Delta T_{ev} + d \cdot \Delta T_{ev}^{\,2} \quad (2)$$

where T_{in} is the air inlet temperature and ΔT_{ev} is the temperature difference between the air inlet temperature and the refrigerant evaporating temperature; the coefficients are: a=-1.696, b=0.009; c=0.898; d=-0.021. In figure 5 two projections of the equation (2) are shown. They represent the trends of the evaporator heating rate with varying the air inlet temperature and the temperature difference between the air inlet temperature and the refrigerant evaporating temperature. It is possible to notice that the effect of the air inlet temperature variation is limited, while, as expected, the temperature difference between the two carrier fluids is more influent.

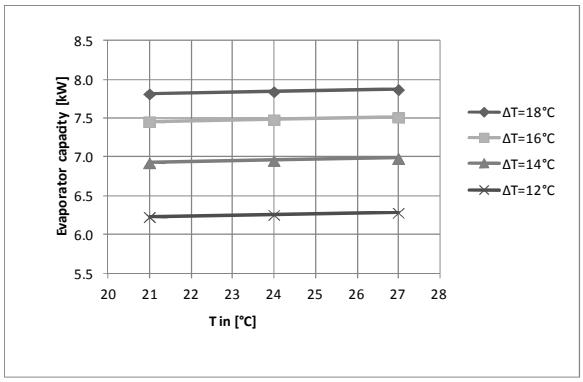

(a)

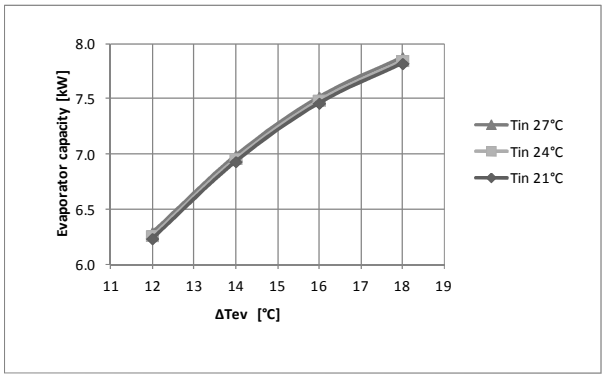

(b)

Figure 5. Evaporator capacity with varying the air inlet temperature, T_{in}, (a) and the temperature difference, ΔT_{ev}, between air and refrigerant evaporating temperature (b).

Moreover, knowing the evaporator capacity, an average overall heat transfer coefficient (UA) for the mini-channel heat exchanger was estimated by means of equations (3) and (4):

$$\dot{P}_{ev} = UA \cdot \Delta T_{ML} \cdot f \quad (3)$$

$$\Delta T_{ML} = \frac{(\Delta T_{ev} - \Delta T_2)}{\ln\left(\frac{\Delta T_{ev}}{\Delta T_2}\right)} \quad (4)$$

where ΔT_{ML} is the logarithmic mean temperature calculated as function of the temperature differences between the two carrier fluids, ΔT_2 and ΔT_{ev}, being ΔT_2 the difference between the air outlet temperature and the refrigerant inlet temperature and ΔT_{ev} the difference between the air inlet temperature and the refrigerant evaporating temperature (figure 6). Such a definition was chosen to approximate the real heat transfer process as much better as possible. The correction factor, f (<1), instead, depends on the fluids inlet and outlet temperatures and on the type of heat exchanger and it takes into account that the heat exchanger is not a counter-current but a cross flow heat exchanger [17]. The obtained UA is equal to 1.158 kW/K with a global uncertainty of 2%.

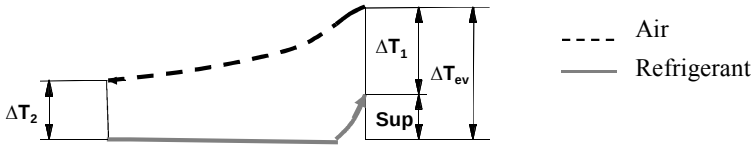

Figure 6. Air and refrigerant temperature trend in the evaporator.

Other tests were conducted with varying the air flow rate (inverter frequency: 20÷27.5 Hz) and a relationship between the evaporator heating rate variation and the air flow rate (ẇ) variation was found:

$$\frac{\Delta \dot{P}_{ev}}{\dot{P}_{ev,0}} = 0.1 \frac{\Delta \dot{w}_{air}}{\dot{w}_{air,0}} \tag{5}$$

the subscript "0" refers to the standard condition at 25Hz. The relation shows that the exchanged power variation is 10% of the air flow rate variation.

3. CFD analysis of the flow field

Main purpose of the numerical simulation of the fluid flow was to analyze the distribution of the two phase refrigerant in the inlet manifold of the evaporator. The CFD analysis was oriented to obtain a first guess solution of the refrigerant flow field, useful to highlight which elements of the actual geometry of the manifold have a greater responsibility in the non optimal distribution of the refrigerant among the multiports.

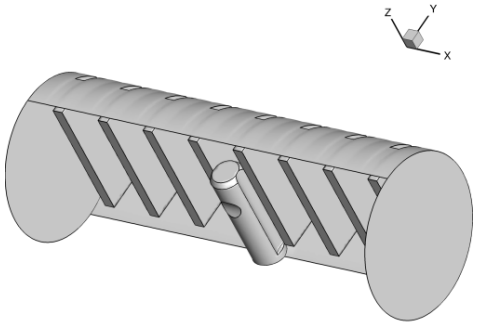

Figure 7. Geometric representation of a portion of the manifold considered in the simulation.

Considering the repetitive pattern around the inlets of the manifold, the computational domain comprises a periodic portion of the manifold, containing only one inlet nozzle and an equal number of multiports for each side (see figure 7). The computational domain was discretized using an unstructured grid of 650.000 nodes: tetrahedral elements were adopted in the core of the fluid volume and a prismatic layer refinement was realized in the near wall region in order to better describe the behavior of the refrigerant entering the multiports channels (Figure 8). The unsteady Reynolds Averaged Navier – Stokes (RANS) equations were solved for the computation of the turbulent flow,

using the SST k-ω turbulence model. Time integration of the fluid flow equations was performed with a time step of 10^{-3} s, in order to produce a second order accurate solution of the flow field. Calculations were assessed by means of the CFD commercial code STAR – CCM+ [18].

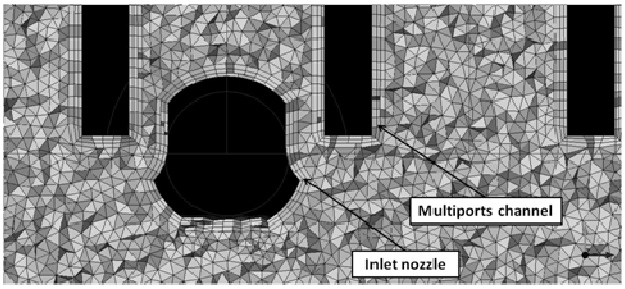

Figure 8. Mesh details in the near wall region

A set of operative conditions, measured during the experimental investigations, were adopted for the numerical model of the refrigerant flow field. The refrigerant, R410A, enters the manifold with a temperature of 276.95 K, a pressure of 0.9 MPa, a quality of 0.359 and a mass flow rate of 165 kg/h, corresponding to an inlet velocity of 6 m/s. Given the pretty high inlet velocity it is possible to consider that the two phase refrigerant flow behaves like a mist [19]. Due to the lack of certainty about the two-phase regime of the refrigerant in this type of application in scientific and technical literature, it was used a simplified approach for modeling the two-phase state of the fluid: this was intended to obtain a first guess reconstruction of the main fluid dynamic structures of the refrigerant flow field in the inlet manifold. Indeed, in the present work, the CFD analysis is aimed at identifying major elements and guidelines to improve the manifold design and achieve a better distribution of the refrigerant among multiports. The adopted model does not reconstruct the interface between liquid and gas phases, assuming equilibrium phase change. The R410A is classified as a quasi-azeotropic mixture, with negligible temperature glide during phase change: thus, it can be modeled as a pure substance. The equation of state of Redlich-Kwong [20] was considered, while the refrigerant thermophysical properties were taken from REFPROP 9.0 database [15].

The numerical results pointed out the symmetry of the flow respect to the inlet nozzle position and, mainly due to the high refrigerant inlet velocity, showed the presence of high vorticity structures among the multiports (figure 9). In figure 9 dark gray areas are associated with fluid moving downward along the vertical direction (negative velocity), thus not contributing to the development of mass flow rate through the multiport inlet sections. This behavior is also evident in terms of the refrigerant mean velocity at the multiports inlet, as shown in figure 10. Indeed a different distribution of the refrigerant between the multiports closer and farther to the inlet nozzle was highlighted: a bigger refrigerant flow passes through the multiports farther from the inlet nozzle (figure 10). Instead, considering a single multiport the flow is higher in the external channels rather than in the inner ones (figure 11).

In order to improve the refrigerant distribution, a new configuration was considered: the inlet nozzle length was reduced while its inlet section was enlarged. This simple modification reduced the inlet velocity of the refrigerant with the advantage of a more uniform distribution of the fluid among the multiports, as shown by the inlet velocity trend in figure 12.

On the basis of the obtained simulation results some conclusions can be drawn to improve the manifold design. In fact the numerical reconstruction of the flow field showed a non homogeneous distribution of the refrigerant into the minichannels and in the different multiports. Possible modifications suggested by such results to improve the distribution could be: reduce the refrigerant inlet velocity, increase the number of inlet nozzles and reduce the protrusion inside the manifold of the multiports closer to the nozzle, in order to reduce the presence of obstacles and stagnation regions in

the manifold. The realization of the latter point needs to be verified from a technical, but mainly, from an economic point of view by the heat exchanger producer.

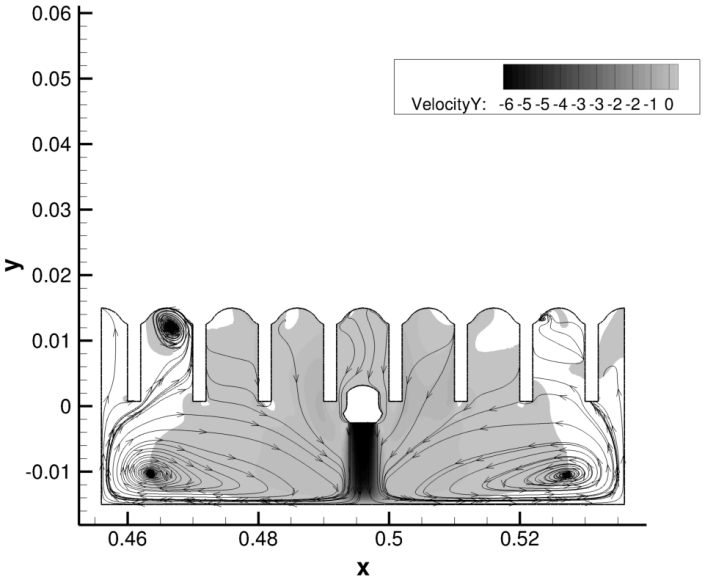

Figure 9. Velocity (m/s) cut-off contour and velocity streamline of the refrigerant in the manifold (view on the vertical middle surface of the manifold).

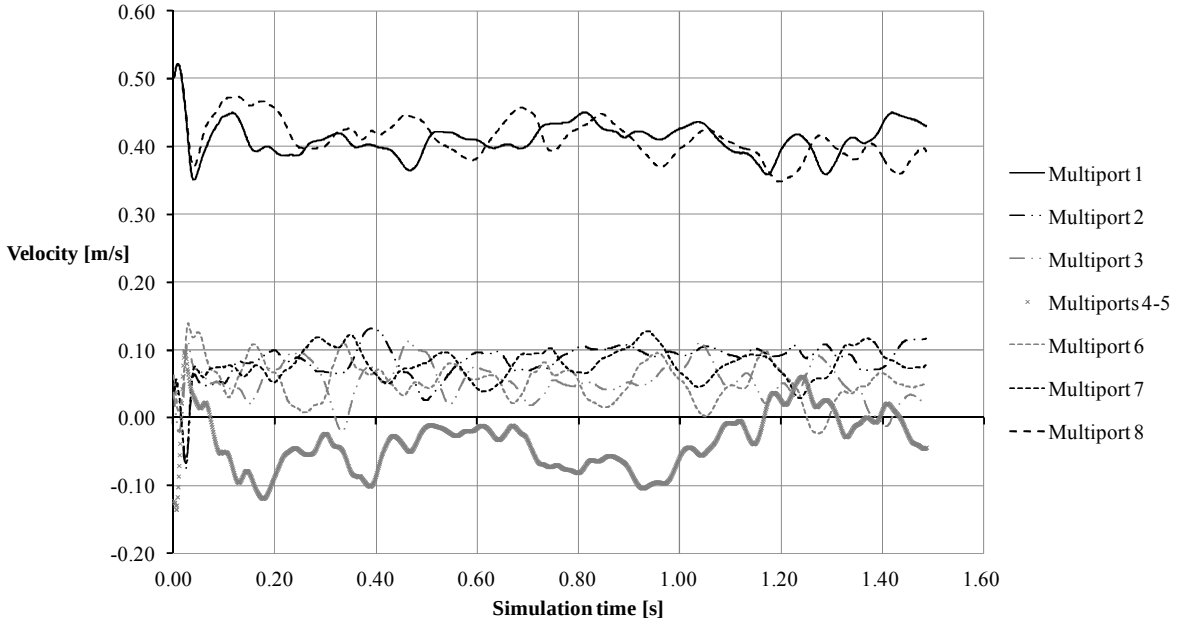

Figure 10. Refrigerant mean velocity (m/s) along the vertical axis (y) at the inlet of the multiports .

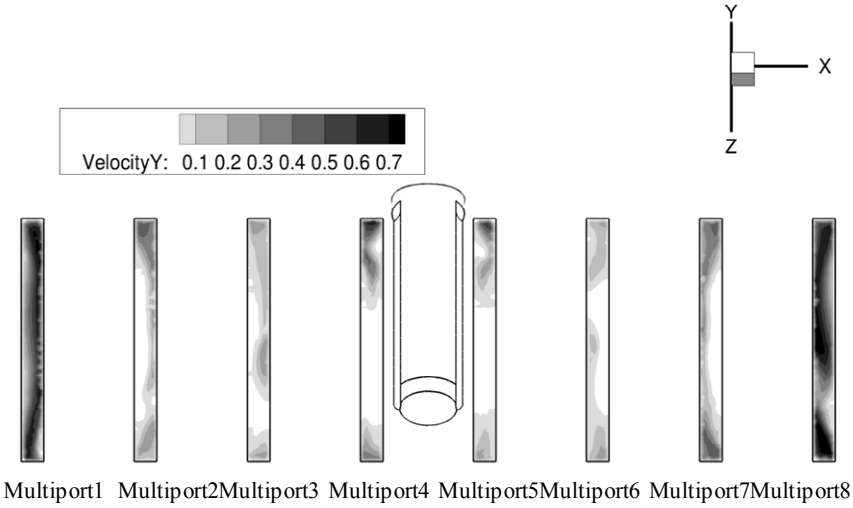

Figure 11. Refrigerant velocity (m/s) cut-off contour on the inlet sections of the multiports.

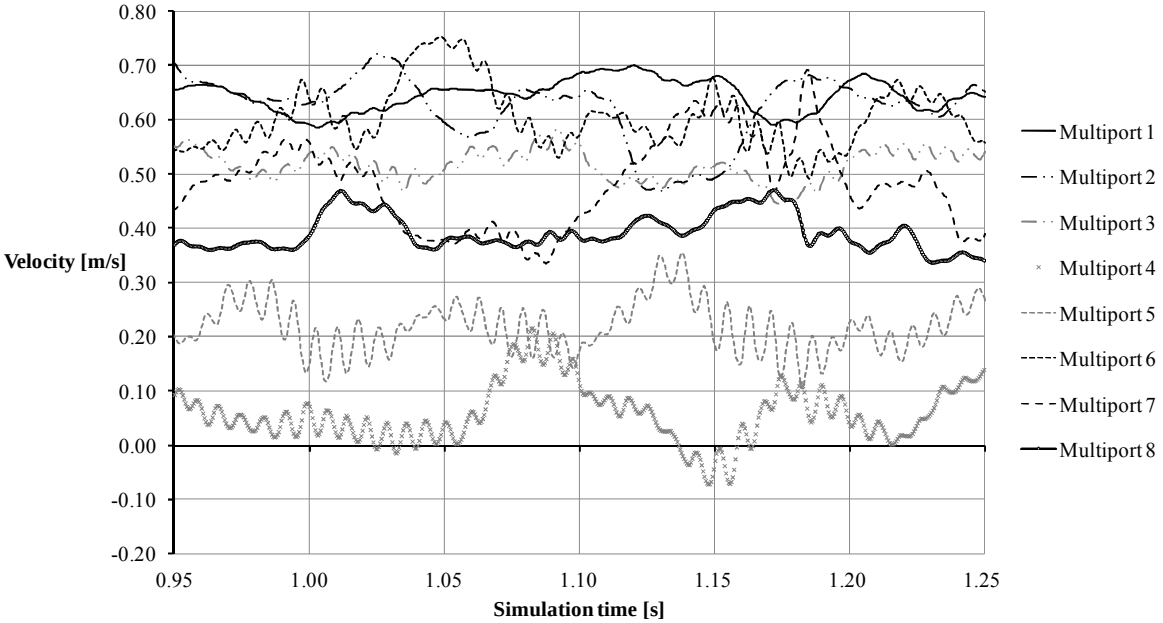

Figure 12. Refrigerant mean velocity (m/s) along the vertical axis (y) at the inlet of the multiports for the manifold with the modified inlet nozzle

4. Conclusions

In this paper a mini-channel heat exchanger used as evaporator in an air-to-air heat pump was studied. The heating rate that can be exchanged was evaluated with varying the inlet fluids conditions. In particular a relationship between such heating rate and the air and refrigerant inlet temperatures was found. Moreover the overall heat transfer capacity was assessed. Eventually, to analyze the role of the inlet manifold for the refrigerant distribution, a CFD study was performed. The obtained results showed a non homogeneous distribution and some hints for the geometry improvement could be drawn. Future developments of this study consist in testing the heat exchanger working as condenser in heating mode and, from the numerical point view, in improving the adopted approach for modeling

the two-phase state of the fluid, by means of methods able to the reconstruct the interface between liquid and gas phases.

Acknowledgement
The authors wish to thank VALMEX for the possibility to study their heat exchanger and present the obtained results.

References

[1] Kandlikar S G 2007 A roadmap for implementing minichannels in refrigeration and air-conditioning systems - Current status and future directions *Heat Transf. Eng.* **28** 973-985
[2] Cavallini A, Del Col D and Rossetto L 2012 Heat transfer and pressure drop of natural refrigerants in minichannels (low charge equipment) *Int. J. Refrig*. **36** 287-300
[3] Alagesan V 2012 Flow boiling heat tranfer in Mini and Micro Channels – A state of the art review *Int. J. Chem. Tech. Res*. **4** 1247-59
[4] Kim S-M and Mudawar I 2013 Universal approach to predicting saturated flow boiling heat transfer in mini/micro-channels – Part II. Two-phase heat transfer coefficient *Int. J. Heat Mass Transf.* **64** 1239–1256
[5] Zhang W, Hibiki T and Mishima K 2004 Correlation for flow boiling heat transfer in mini-channels *Int. J. Heat Mass Transf.* **47** 5749–5763
[6] Sun L and Mishima K 2009 Evaluation analysis of prediction methods for two-phase flow pressure drop in mini-channels *Int. J. Multiph. Flow* **35** 47–54
[7] Cheng L and Mewes D 2006 Review of two-phase flow and flow boiling of mixtures in small and mini channels *Int. J. Multiph. Flow* **32** 183–207
[8] Brix W, Kærn RM and Elmegaard B 2010 Modelling distribution of evaporating CO_2 in parallel minichannels *Int. J. Refrig*. **33** 1086-94
[9] Kulkarni T, Bullard CW and Cho K 2004 Header design tradeoffs in microchannel evaporators *Appl. Therm. Eng*. **24** 759-76
[10] Kim N-H, Lee E-J and Byun H-W 2012 Two-phase refrigerant distribution in a parallel flow minichannel heat exchanger having horizontal headers *Int. J. Heat Transf.* **55** 7747–59
[11] Kim N-H, Kim D-Y and Byun H-W 2011 Effect of inlet configuration on the refrigerant distribution in a parallel flow minichannel heat exchanger *Int. J. Refrig*. **34** 1209-21
[12] Qi Z, Chen J and Radermacher R 2009 Investigating performance of new mini-channel evaporators *App. Therm. Eng*. **29** 3561–67
[13] Choi JM, Payne WV and Domanski PA 2003 Effects of nonuniform refrigerant and airflow distribution of finned-tube evaporator performance *Proc. Int. Cong. Refrig.* Washington DC, USA, ICR0040
[14] Selleri T, Najafi B, Rinaldi F and Colombo G 2013 Mathematical modeling and multi-objective optimization of a mini-channel heat exchanger via genetic algorithm *J. Therm. Sci. Eng. Appl.* **5** (3) 10p
[15] REFPROP 9.0 2010 NIST Reference Fluid Thermodynamic and Transport Properties Database
[16] Lemmon EW and Jacobsen RT 2004 Equations of State for Mixtures of R-32, R-125, R-134a, R-143a, and R-152a *J. Phys. Chem. Ref. Data* **33** 593-620
[17] Guglielmini G and Pisoni C 1990 *Elementi di trasmissione del calore* (Milan: Editore Veschi).
[18] STAR - CCM+ 2012 User Guide release 7.04. CD – Adapco
[19] Webb RL and Chung K 2004 Two-phase flow distribution in tubes of parallel flow heat exchangers *Heat Transf. Eng.* **26** 3-18
[20] Redlich O and Kwong JNS 1949 On The Thermodynamics of Solutions *Chem. Rev.* **44** 233–44